Electronic Supplementary Material (ESI) for Organic Chemistry Frontiers.

Assigning the stereochemical structures of aurantinin A and B with the assistance of biosynthetic investigations

Dacheng Wang,[a,‡] Pengwei Li,[a,‡] Jialei Yan,[c] Huijin Mao,[a,b] Lilu Liu,[a,b] Min Wang,[a,c] Meng Chen,[a,b] Tao Ye,[c,d,†] and Yihua Chen[a,b,†]

State Key Laboratory of Microbial Resources, Institute of Microbiology, Chinese Academy of Sciences, Beijing 100101, China.

University of Chinese Academy of Sciences, Beijing 100049, China.

Innovation Center of Marine Biotechnology and Pharmaceuticals, School of Biotechnology and Health Sciences, Wuyi University, Jiangmen 529020, Guangdong, China.

State Key Laboratory of Chemical Oncogenomics, Peking University Shenzhen Graduate School, Xili, Nanshan District, Shenzhen 518055, China.

Contents

Experimental methods

DNA manipulation and sequence analysis. General DNA manipulations were performed as described.[1] The primers used in this study (listed in Table S1) were synthesized by Generay Co. (Shanghai, China). The PCR enzymes PrimeSTAR DNA polymerase (Takara, Japan) or Taq DNA polymerase (TransGene, Beijing, China) were used for DNA amplification according to the manufacturers' instructions. DNA sequencing was performed by TianYi HuiYuan Co. (Beijing, China). Electroporation of *B. subtilis* fmb60 was performed with an established protocol except the electric pulse condition was modified to 15 kV/cm, 1 kΩ, and 25 μF.[2] Gene function annotation and multiple alignment of protein sequences were performed with BLAST (http://www.ncbi.nlm.nih.gov/blast) and CLUSTALW (https://www.ebi.ac.uk/Tools/msa/clustalw2/), respectively.

Construction of *B. subtilis* Δ*art24*. To construct the gene in-frame deletion mutant *B. subtilis* Δ*art24*, two 1.0-kb DNA fragments flanking the *art24* gene were amplified with primer pairs 24-L-F/24-L-R and 24-R-F/24-R-R, respectively. Plasmid pRN5101::*art24*-UD was generated by inserting the two 1.0-kb fragments into the *Hin*dIII site of pRN5101 using one-step cloning strategy.[3] After introducing pRN5101::*art24*-UD into *B. subtilis* fmb60 by electroporation, the erythromycin resistant transformants were selected as the single-crossover mutants, and then cultured in LB without antibiotics at 37 °C overnight to induce the second crossover. The erythromycin sensitive colonies were screened out by replicating them on plates with or without erythromycin. The selected colonies were verified as the desired *B. subtilis* Δ*art24* mutants by PCR analysis with primer pair 24-L-F/24-R-R, and then confirmed by sequencing the size-correct amplicons.

Protein expression and purification. For the expression of Art24 (WP_069149234) in *E. coli*, the 1.2-kb *art24* gene was cloned by PCR using the genomic DNA of *B. subtilis* fmb60 as a template with primer pair 28-24-F/28-24-R and inserted into the *Nde*I and *Bam*HI sites of pET28a to afford pET28a::*art24*. Gene *tyl1a* was synthesized and cloned into pET28a to generate pET28a::*tyl1a* by Generay (Shanghai, China).[4]

E. coli BL21 (DE3) transformant harboring the protein expression plasmid (pET28a::*art24* or pET28a::*tyl1a*) was inoculated into LB with 50 μg/mL kanamycin and cultured at 37 °C, 220 rpm. The overnight culture was used to inoculate LB with 50 μg/mL kanamycin (1%, v/v) and incubated at 37 °C, 220 rpm until OD_{600} reaching 0.6. Expression of Art24 or Tyl1a was then induced by the addition of isopropyl-β-thiogalactoside (IPTG) at a final concentration of 0.1 mM. After cultured at 16 °C, 220 rpm for 18 hours, the cells were harvested by centrifugation, re-suspended in lysis buffer (20 mM Tris-HCl, 500 mM NaCl, 5 mM imidazole, pH 7.9), and burst by sonication. The cell debris was then removed by centrifugation and the supernatant was loaded onto a Ni-NTA affinity column well equilibrated using lysis buffer, and then washed with washing buffer (20 mM Tris-HCl, 500 mM NaCl, 60 mM imidazole, pH 7.9) followed by elution buffer (20 mM Tris-HCl, 500 mM NaCl, 500 mM imidazole, pH 7.9). The desired fractions were combined, desalted using PD10 column, concentrated by ultracentrifugation with an Amicon Ultra centrifugal filter (Millipore, MA, USA; molecular mass cutoff of 10 kDa), and stored in 25 mM HEPES (pH 7.5) buffer with 20% glycerol at -80 °C. Protein concentrations were measured by the Bradford assay.[5]

Art24 assay. The 50 μL reaction mixture consisted of 25 mM HEPES (pH 7.5), 1mM $MgCl_2$, 1 mM ART A, 1 mM TDP-3-keto-6-deoxy-α-D-glucose and 5 μM Art24. The reaction was performed at 30 °C for 2 hours before it was quenched by adding an equal volume of acetonitrile. After centrifugation, the supernatant was analyzed by HPLC and MS.

Spectroscopic analysis. HPLC analysis of ARTs was carried out with an Apollo C18 column (5 μm, 4.6 mm × 250 mm, Alltech, IL, USA) on a Shimadzu HPLC system (Shimadzu, Kyoto, Japan). The detection wavelength was 280 nm. The column was developed with acetonitrile and water containing 0.1% formic acid at a flow rate of 0.8 mL/min. Percentage of acetonitrile was changed using the following gradient: 0-32 min, 30% to 65%; 32-33 min, 65% to 100%; 33-38 min, 100%; 38-39 min, 100%-30%; 39-45 min, 30%.

Production and isolation of ART A and B. For the production of ART A, *B. subtilis* Δ*art24* mutant was cultured

in medium BPY (0.5% beef extract, 1.0% peptone, 0.5% yeast extract, 1% glucose, 0.5% NaCl, pH 7.0) as described.[6] The well-prepared seed culture was inoculated (3% v/v) into the production medium (Landy medium: 4.2% glucose, 1.4% L-sodium glutamate, 0.05% $MgSO_4$, 0.05% KCl, 0.1% KH_2PO_4, 0.0015% $FeSO_4$, 0.005% $MnSO_4$, 0.0016% $CuSO_4$, pH 7.0) and cultured at 33 °C, 200 rpm for 36 h. After centrifugation, the cell debris was discarded and the supernatant was collected and subjected to Diaion HP20 macroporous resin. After being eluted with methanol and concentrated at 25 °C *in vacuo*, the extract was subjected to a silica gel column (600 g, 200-300 mesh, 6.5 cm × 110 cm), which was developed sequentially using 4 L each of petroleum ether, petroleum-ethyl acetate (50/50, v/v), ethyl acetate, ethyl acetate-methanol (50/50, v/v), and methanol. The ethyl acetate fractions containing ART A were concentrated *in vacuo* and then subjected to a reversed-phased C18 column (3.0 cm × 150 cm) that was eluted with acetonitrile/water gradient (40/60, 48/52, 75/25, and 90/10, v/v) sequentially. The fractions containing ART A were concentrated *in vacuo* and refined by semi-preparative HPLC (Zorbax SB-C18, 5 μm, 9.4 mm × 250 mm, Agilent, CA, USA). The column was eluted with acetonitrile/water (50/50, v/v) containing 0.1% formic acid at a flow rate of 3.5 mL/min. About 8.0 mg ART A was obtained from 60 L *B. subtilis* Δ*art24* culture.

ART B was produced and isolated using the same procedures as those of ART A, except that the wild type strain *B. subtilis* fmb60 was the producer and the semi-preparative HPLC column was eluted with acetonitrile/water (47/53) containing 0.1% formic acid at a flow rate of 3.5 mL/min. About 6 mg ART B was obtained from 120 L *B. subtilis* fmb60 culture.

Computational methods. Both energy minimization and conformational analysis of ART A were carried out with the Conflex 7.0a software using built-in MMFF94 force field.[7] For ***NMR calculation***, optimization and frequency analyses for conformers were carried out using dispersion corrected density functional theory (DFT-D3BJ) at b3lyp/6-311G(d, p) level.[8] Calculations of ^{13}C NMR chemical-shift (shielding tensors values) were performed at the mPW1PW91/6–311+G(2d,p) level with IEFPCM solvent model using DMSO as solvent. The DP4+ statistical

analysis was then carried out using the DP4+ excel file under the instructions provided by Sarotti's laboratory.[9] For ***ECD calculation***, optimization and frequency analyses for conformers were carried out using dispersion corrected density functional theory (DFT-D3BJ) at b3lyp/6-311G(d, p) level with tight convergence criteria, and with IEFPCM solvent model using methanol as a solvent. The electronic circular dichroism (ECD) were calculated using the time-dependent density-functional theory (TD-DFT) method at b3lyp/6-311G(d, p) level with the IEFPCM solvent (methanol) model. All the optimization and frequency analyses for NMR and ECD calculation of conformers were executed with Gaussian9 software. The Boltzmann distribution and Gibbs free energy at 298.15 K of conformers were generated according to the analyses of Gaussian9 output files by Shermo 2.3 software.[10]

Reference

1. Sambrook, J., Russell, D. Molecular Cloning: A Laboratory Manual, Third Edition; Cold Spring Harbor Laboratory Press: Cold Spring Harbor, New York 2001.
2. Matsuno, Y., Ano, T., Shoda, M. High-efficiency transformation of *Bacillus subtilis* NB22, an antifungal antibiotic iturin producer, by electroporation. *J. Biosci. Bioeng.* 1992, **73**, 261-264.
3. Zhang, L. Teng, K., Wang, J., Zhang, Z., Zhang, J., Sun, S., Li, L., Yang, X., Zhong, J. CerR, a single-domain regulatory protein of the LuxR family, promotes cerecidin production and immunity in *Bacillus cereus*. *Appl. Environ. Microbiol.* 2018, **84**, e02245-17.
4. Melançon, C, Hong, L., White, J., Liu, Y., Liu, H. Characterization of TDP-4-keto-6-deoxy-D-glucose-3,4-ketoisomerase from the D-mycaminose biosynthetic pathway of *Streptomyces fradiae*: In vitro activity and substrate specificity studies. *Biochemistry* 2007, **46**, 577-590.
5. Bradford, M. A rapid and sensitive method for the quantitation of microgram quantities of protein utilizing the principle of protein-dye binding. *Anal. Biochem.* 1976, **72**, 248-254.
6. Yang, J., Zhu, X., Cao, M., Wang, C., Zhang, C., Lu, Z., Lu, F. Genomics-inspired discovery of three antibacterial active metabolites, aurantinins B, C, and D from compost-associated *Bacillus subtilis* fmb60. *J. Agric. Food Chem.* 2016, **64**, 8811-8820.
7. Goto, H., Ohta, K., Kamakura, T., Obata, S., Nakayama, N., Matsumoto, T., Osawa, E. Conflex version 7.0. *Tokyo. Conflex Corp* 2013.

8. Grimme, S., Ehrlich, S., Goerigk, L. Effect of the damping function in dispersion corrected density functional theory. *J. Comput. Chem.* 2011, **32**, 1456–1465.
9. Grimblat, N., Zanardi, M., Sarotti, A. Beyond DP4: an improved probability for the stereochemical assignment of isomeric compounds using quantum chemical calculations of NMR shifts. *J. Org. Chem.* 2015, **80**, 12526–12534.
10. Lu, T., Chen, Q. Shermo: A general code for calculating molecular thermochemistry properties. *Comput. Theor. Chem.* 2021, **1200**, 113249.

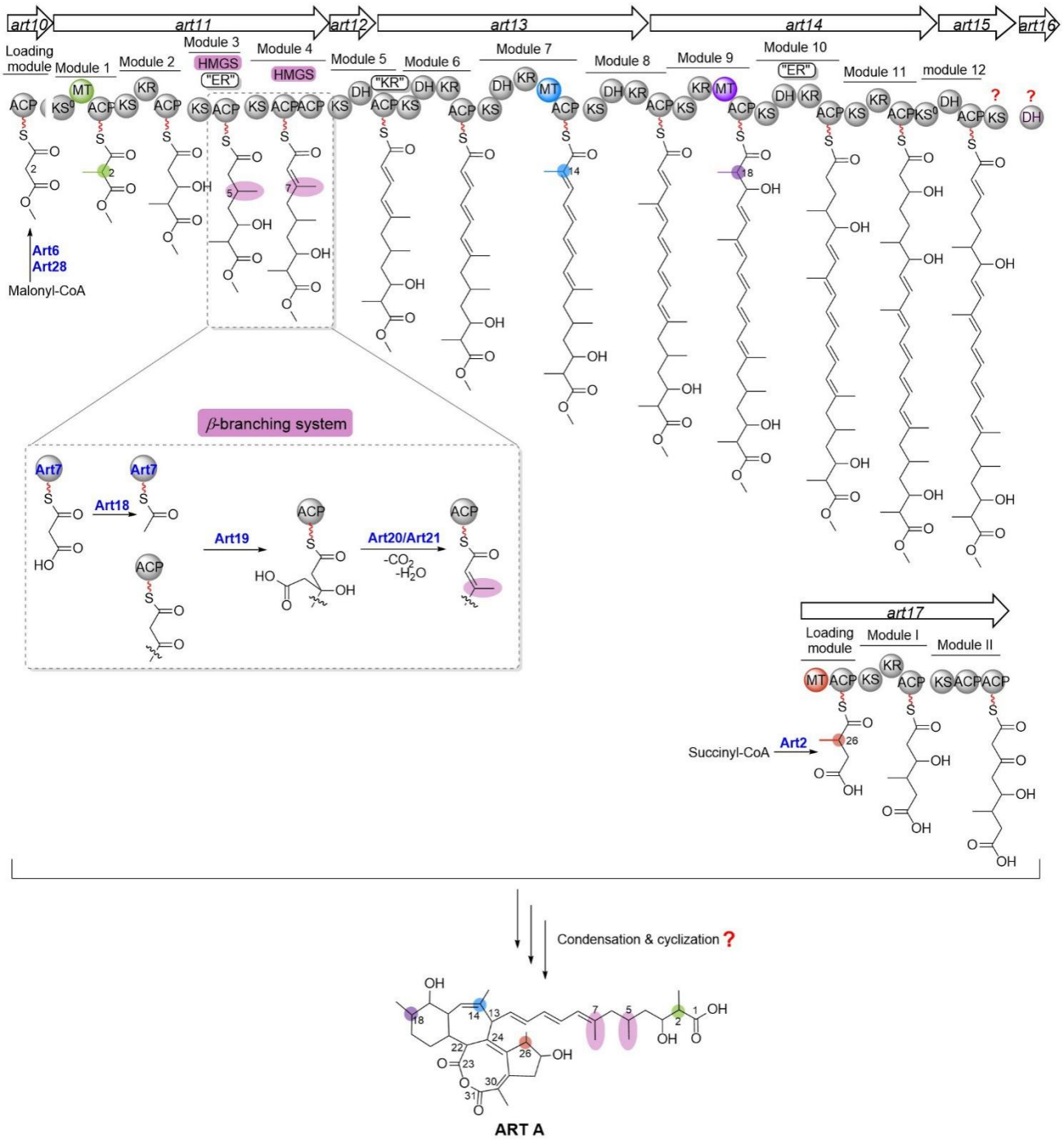

Fig. S1 The proposed biosynthetic pathway of ART A. The methyl groups at C-2, C-14, C-18, and C-26 are highlighted with points in green, blue, purple, and brown, respectively; the methyltransferase domains Art11MT, Art13MT, Art14MT, and Art17MT are marked with the same color as the corresponding methyl group. The inset depicts the process that methyl groups are appended to C-5 and C-7 of the ACP-bound intermediates by *β*-branching system. ACP, acyl carrier protein; KS, ketosynthase; KS^0, non-elongating ketosynthase; KR, ketoreductase; DH, dehydratase; ER, enoylreductase; MT, methyltransferase; HMGS, hydroxymethylglutaryl synthase.

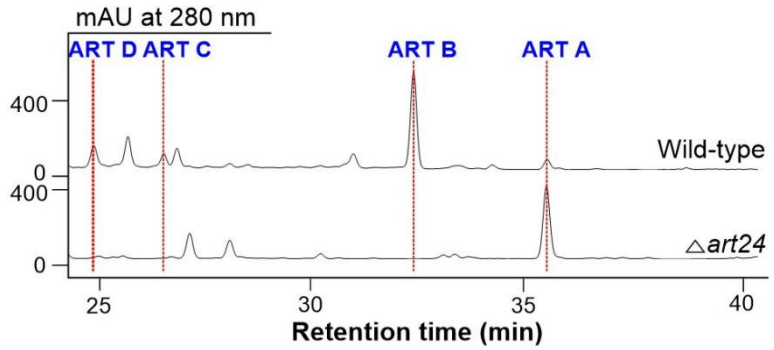

Fig. S2 HPLC profiles of *B. subtilis* fmb60 wild-type and the mutant strain Δ*art24*.

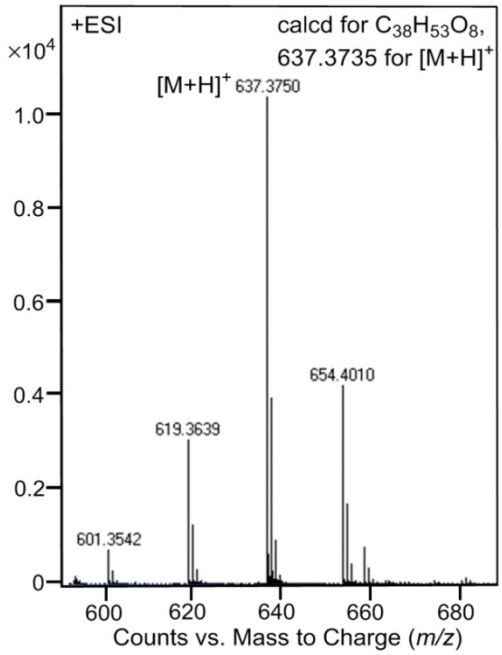

Fig. S3 HRESIMS spectrum of ART A.

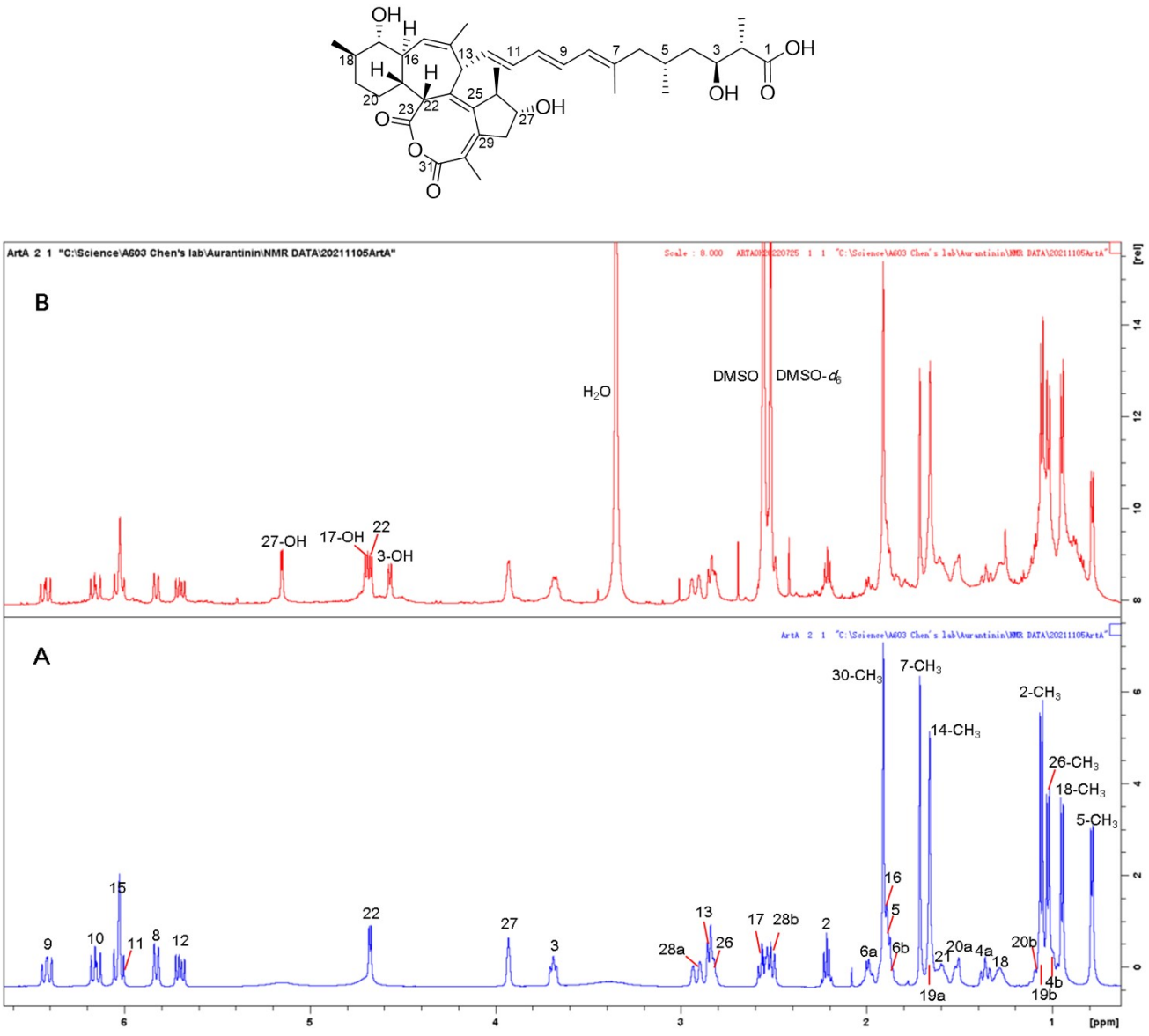

Fig. S4 ^{1}H NMR spectra (500 MHz) of ART A. (A) ^{1}H NMR spectrum (500 MHz) of ART A in DMSO-d_6; **(B)** ^{1}H NMR spectrum (500 MHz) of ART A in DMSO-d_6 with a touch of DMSO, under which condition the signals of hydroxyl protons were clearly visualized. Therefore, this NMR condition was used in the following COSY and ROSEY analyses when the correlations of the hydroxyl protons needed to be considered.

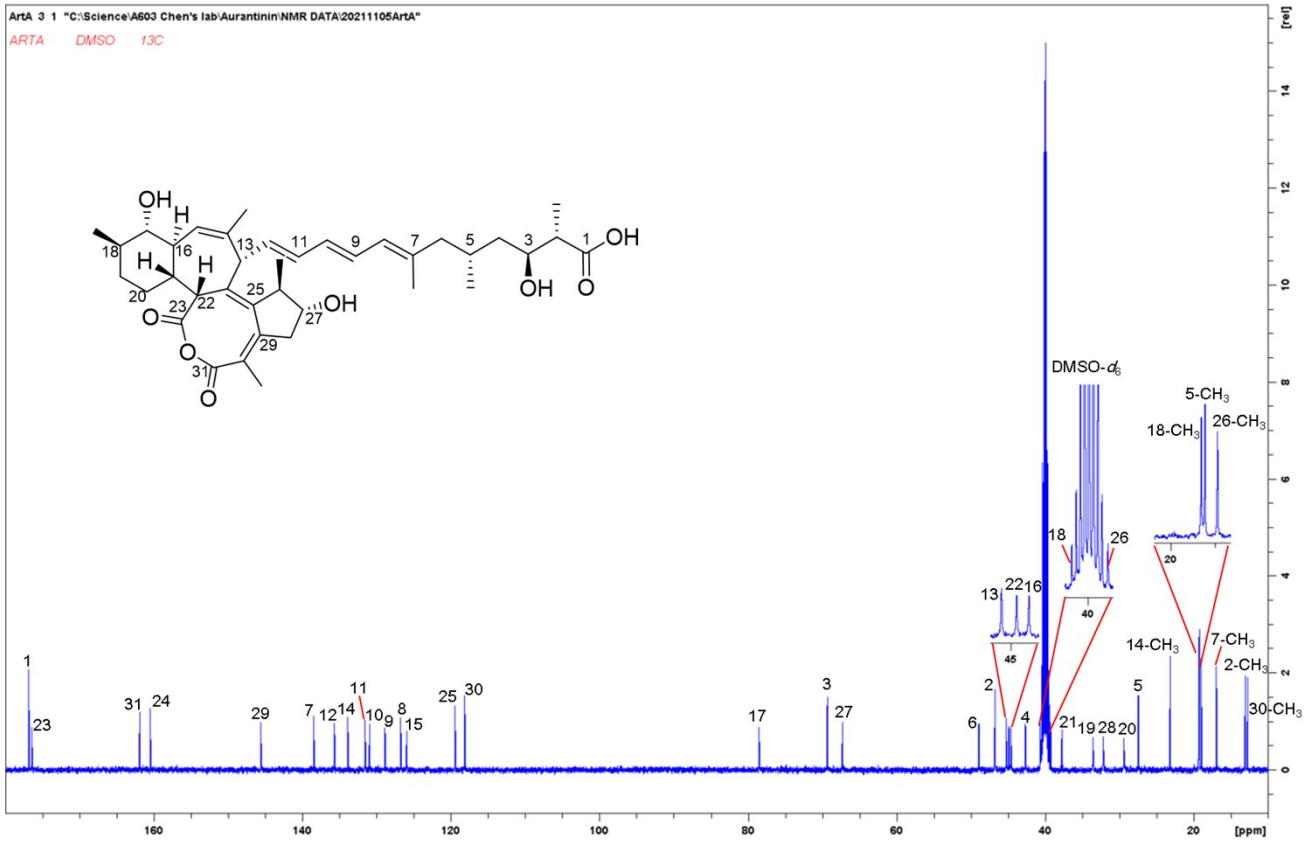

Fig. S5 ^{13}C NMR spectrum (125 MHz) of ART A in DMSO-d_6.

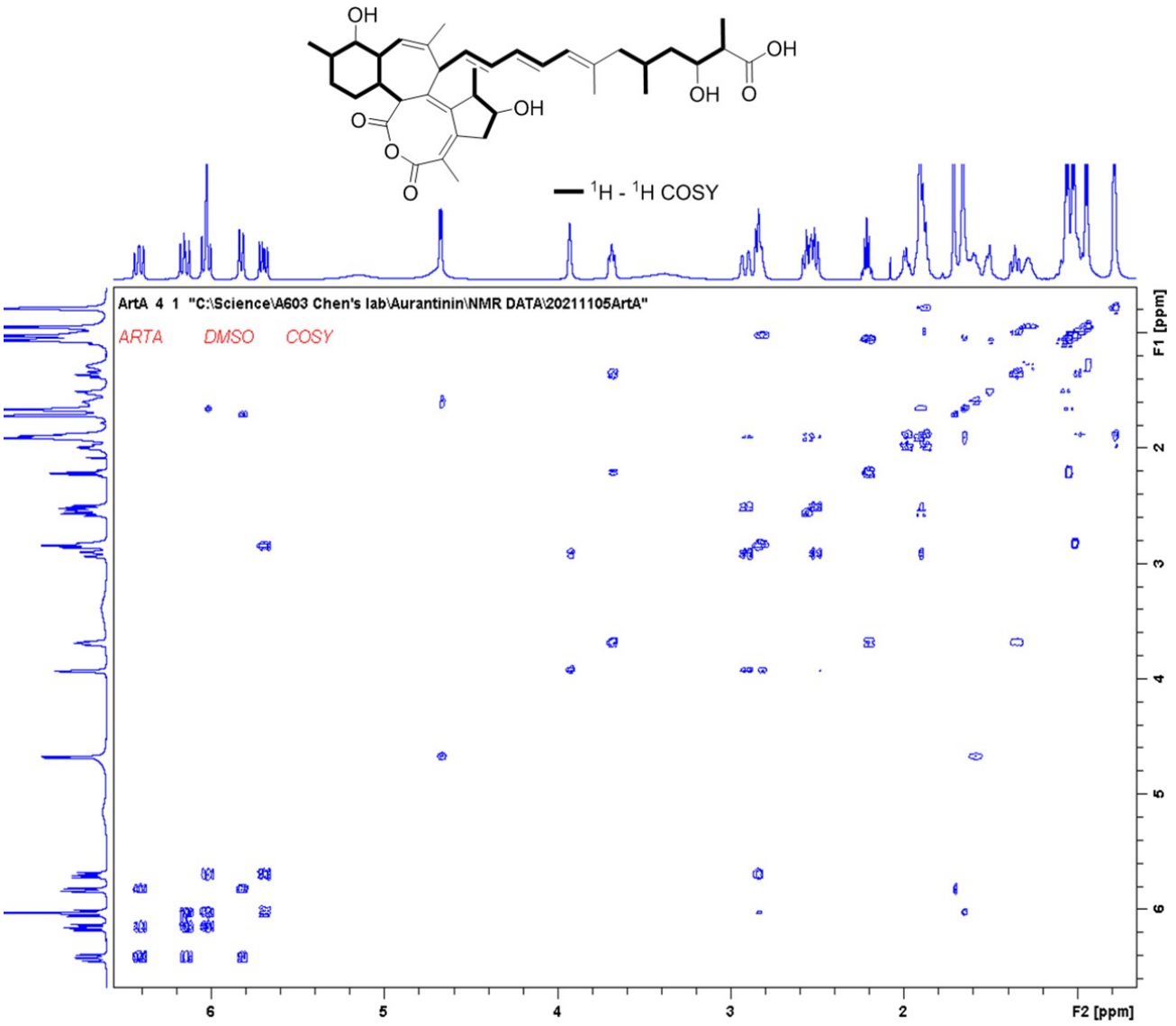

Fig. S6 ^{1}H-^{1}H COSY spectrum (500 MHz) of ART A in DMSO-d_6.

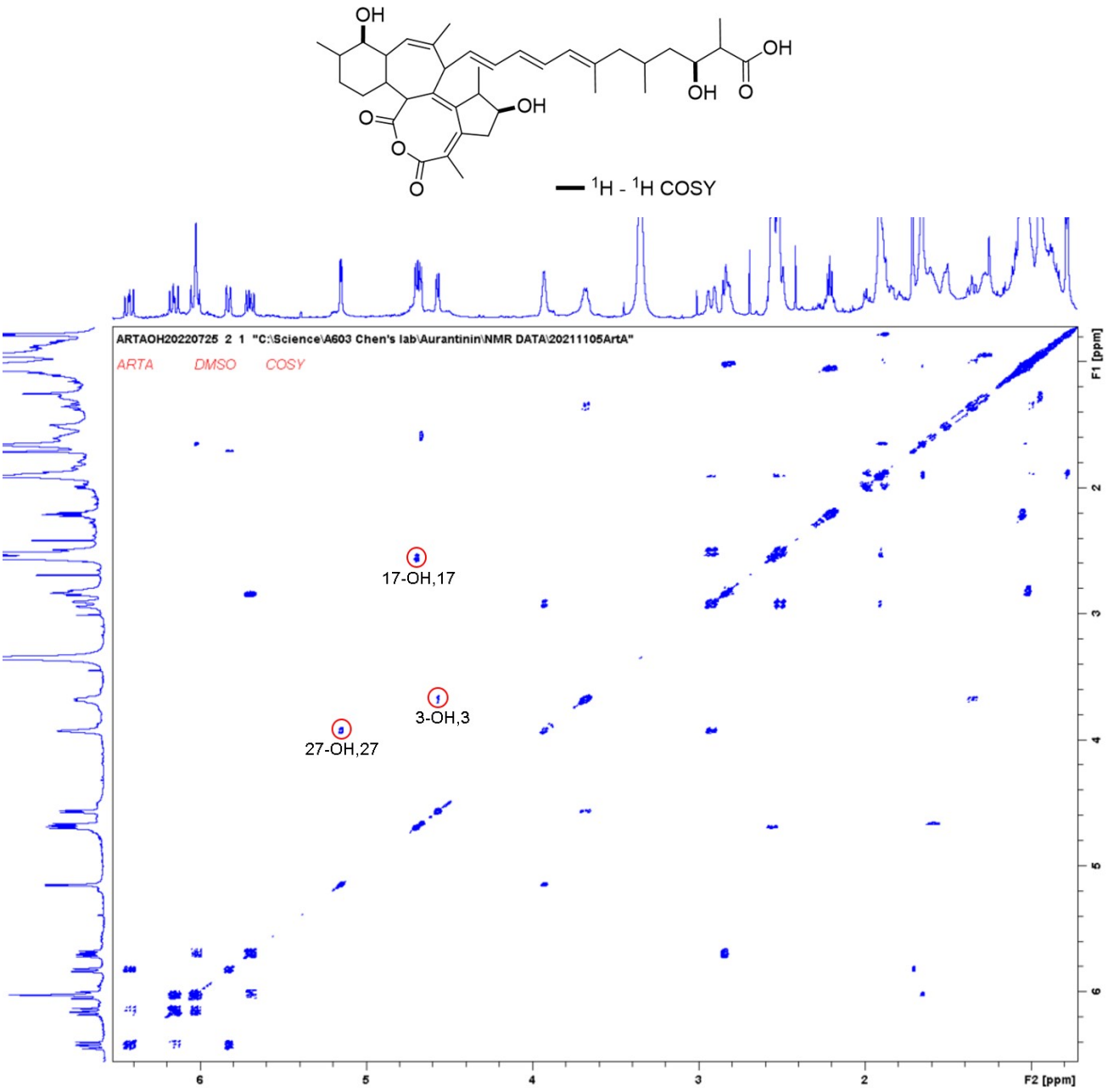

Fig. S7 ^{1}H-^{1}H COSY spectrum (500 MHz) of ART A in DMSO-d_6 with a touch of DMSO.

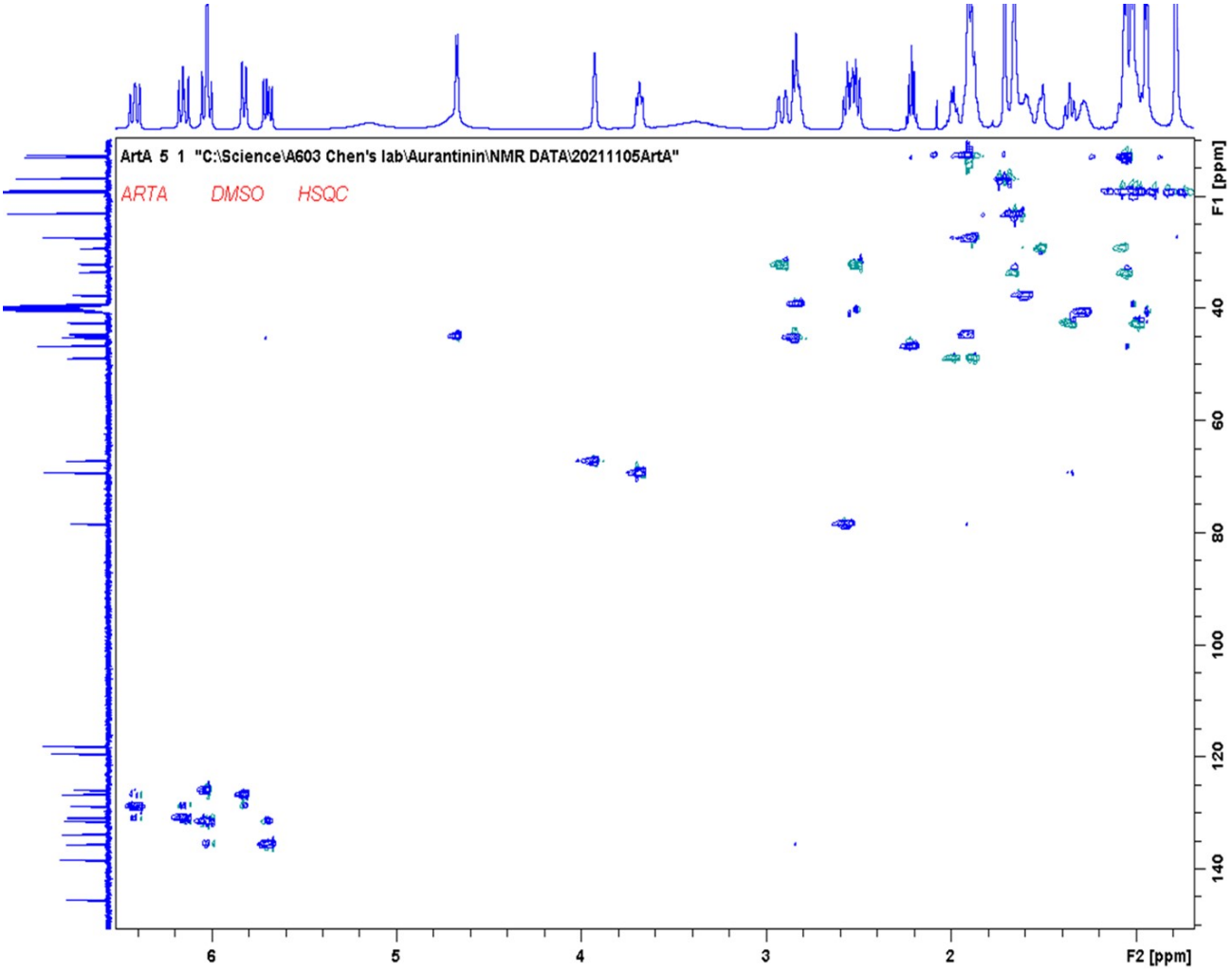

Fig. S8 ^{1}H-^{13}C HSQC spectrum (500 MHz) of ART A in DMSO-d_6.

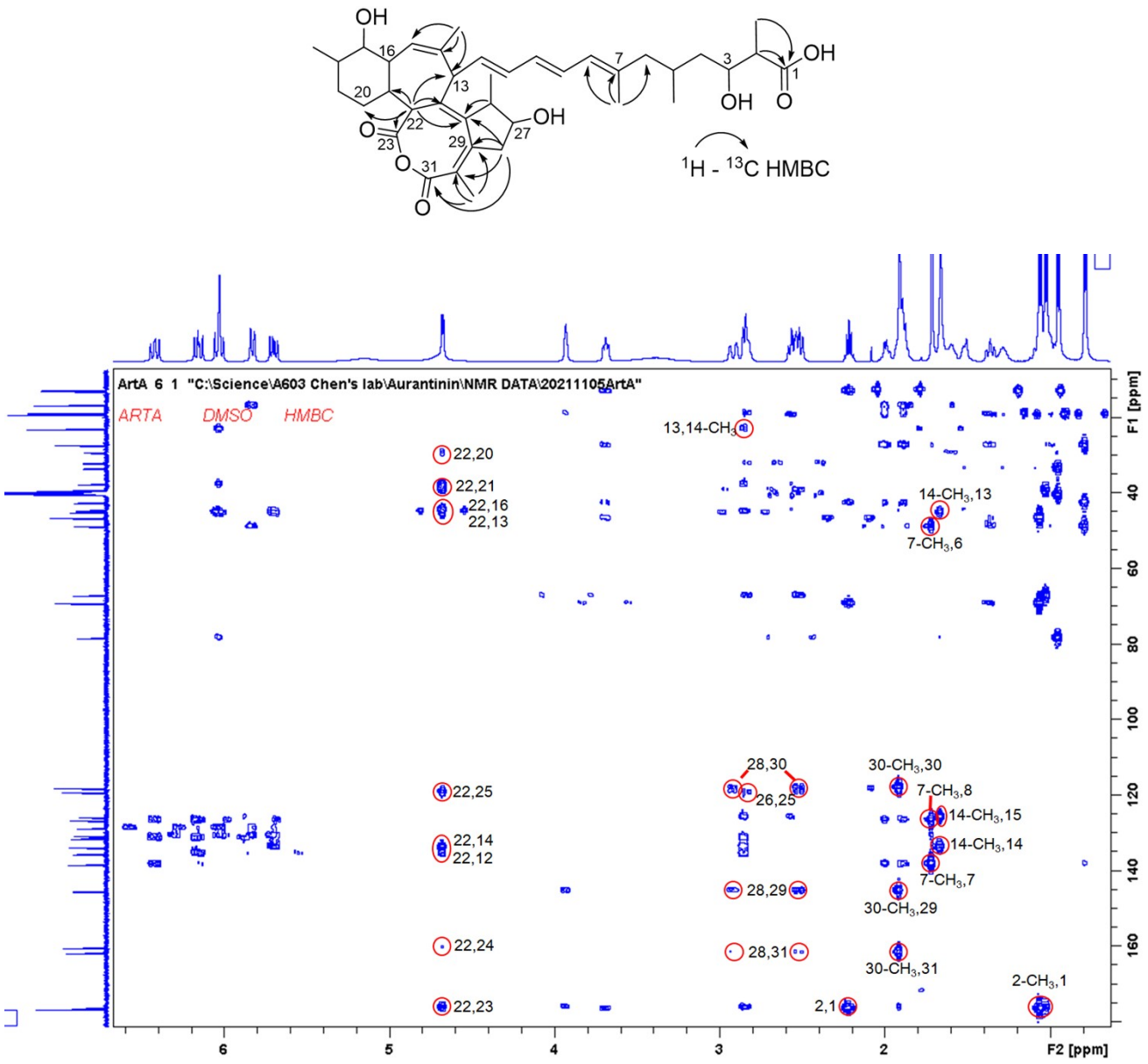

Fig. S9 ^{1}H-^{13}C HMBC spectrum (500 MHz) of ART A in DMSO-d_6.

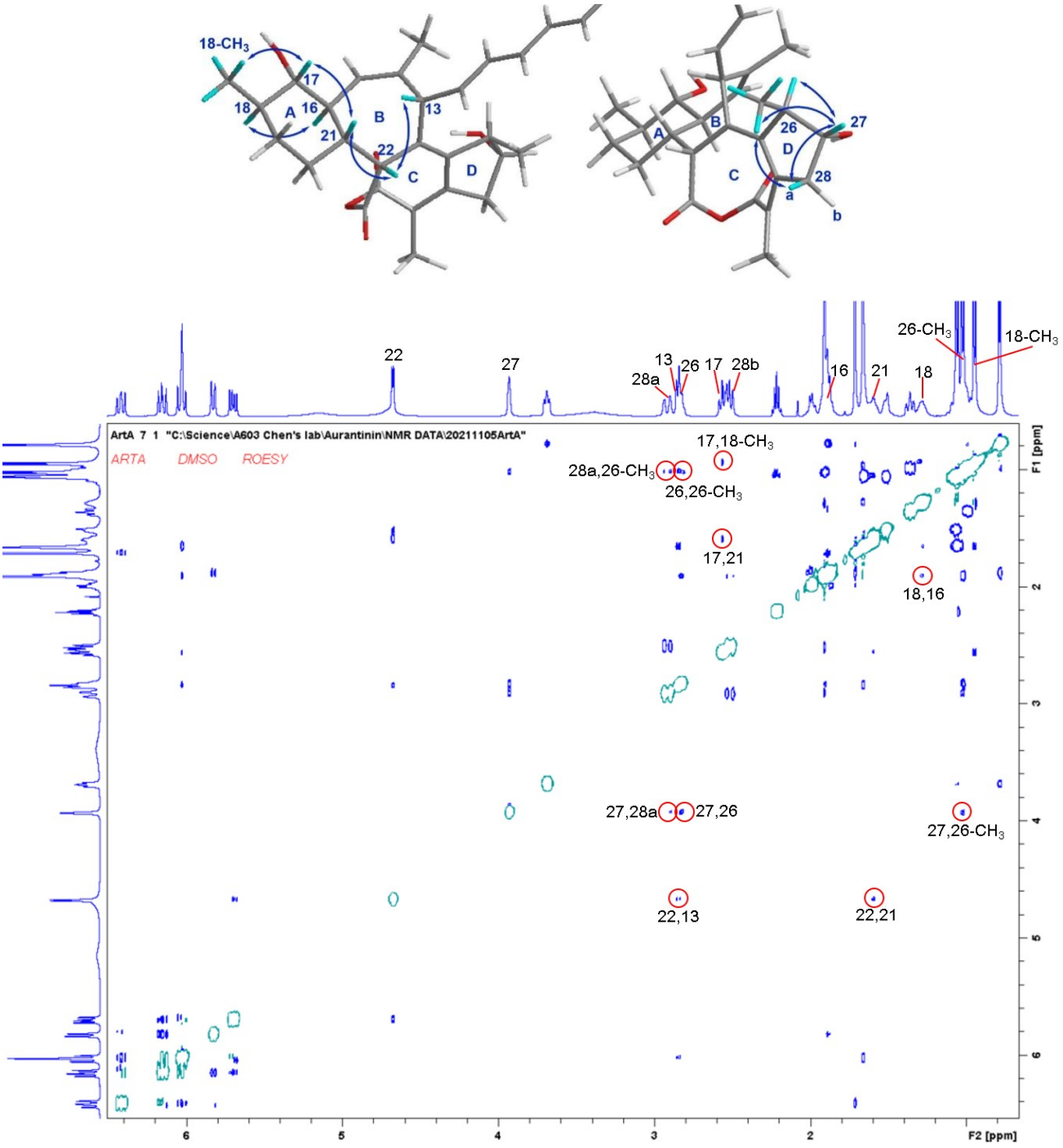

Fig. S10 ^{1}H-^{1}H ROESY spectrum (500 MHz) of ART A in DMSO-d_6.

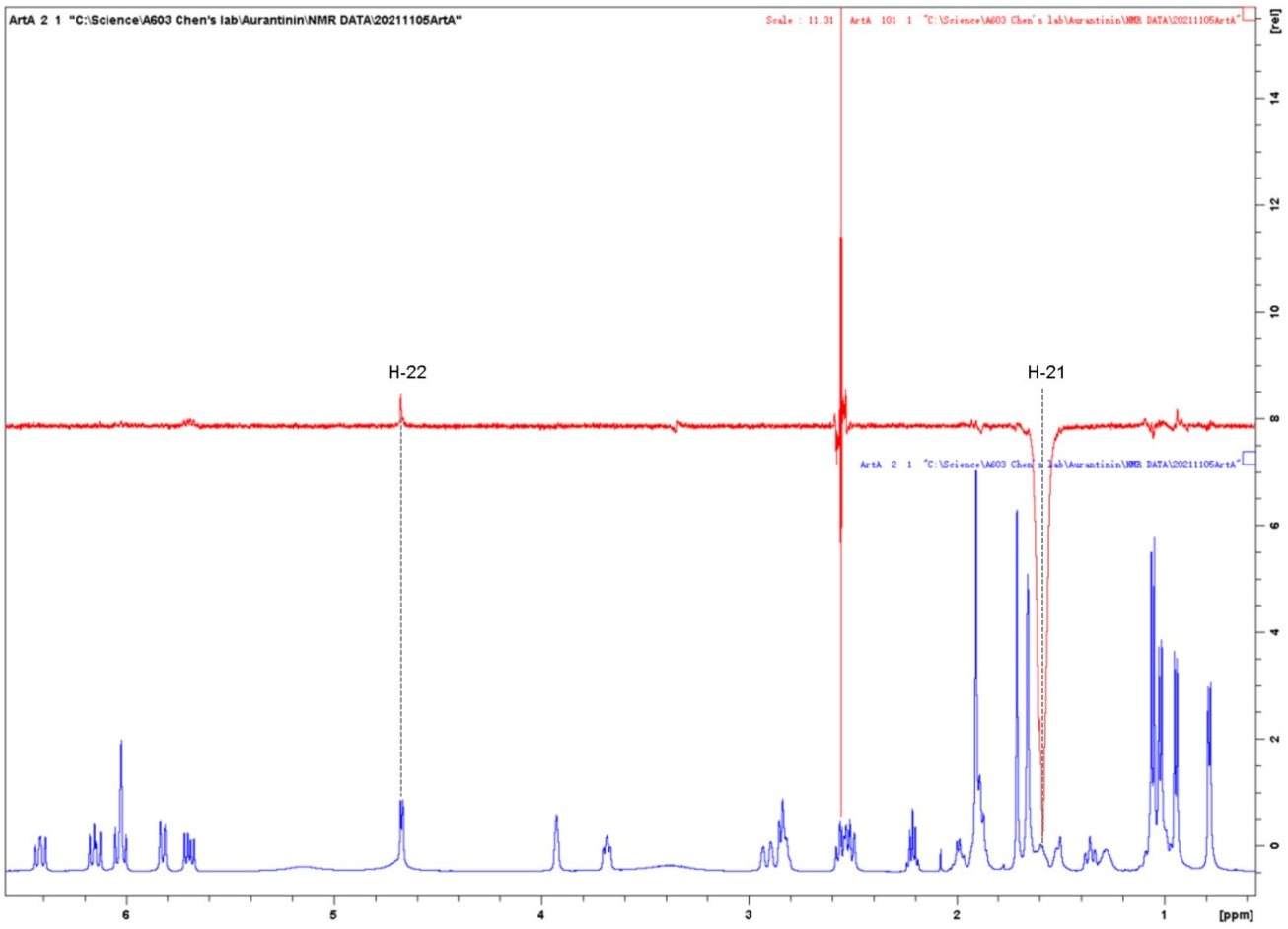

Fig. S11 1D ROESY spectrum (500 MHz) of the H-21 of ART A in DMSO-d_6. The ^{1}H NMR spectrum (500 MHz) of ART A in DMSO-d_6 is also presented as a reference. 1D ROESY experiment parameters were set as: SW 20 ppm; O1P 8.0 ppm; D1 1 sec; D16 0.0002 sec; P15 0.2 sec; NS 128.

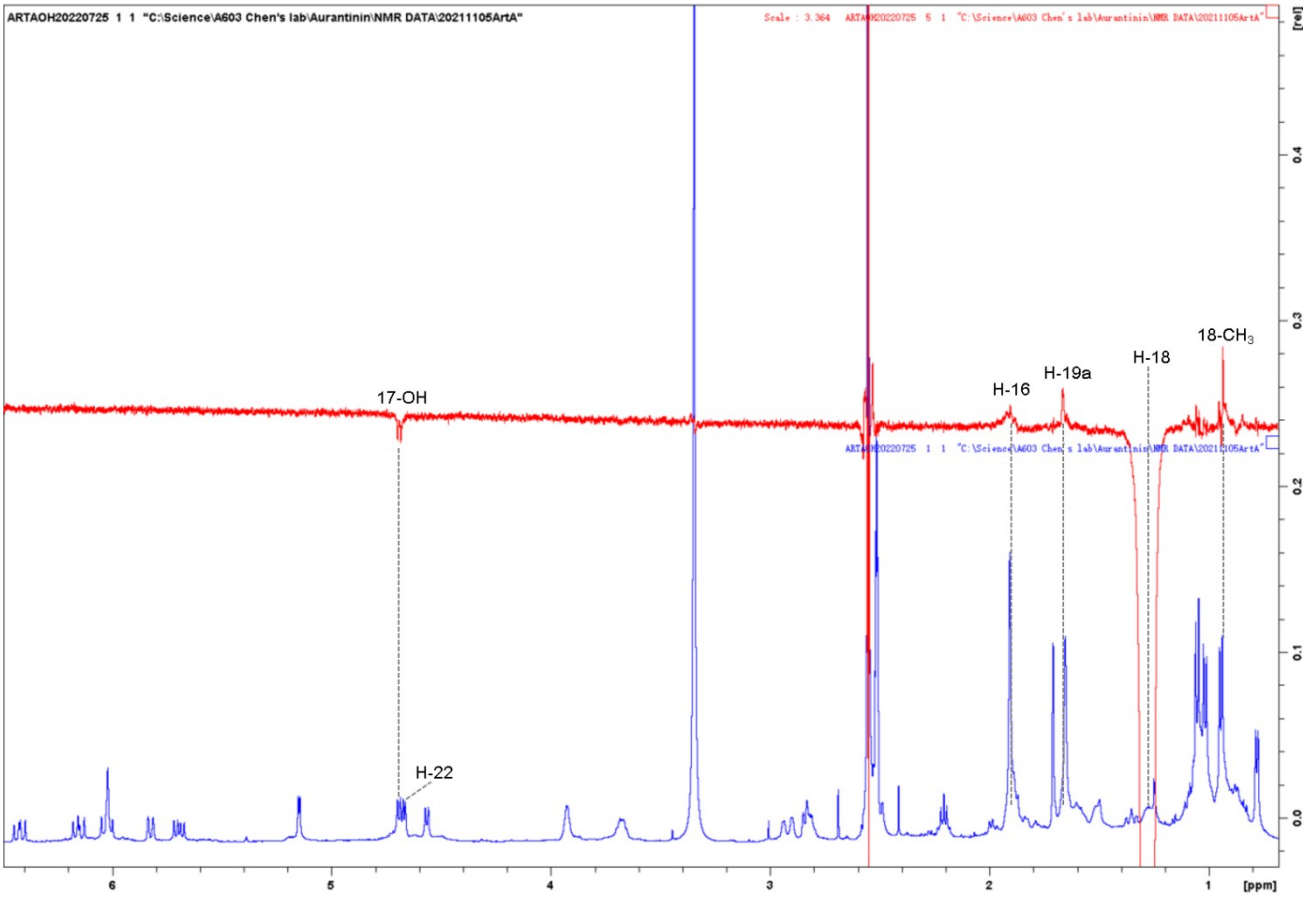

Fig. S12 1D ROESY spectrum (500 MHz) of the H-18 of ART A in DMSO-d_6 with a touch of DMSO. The ^{1}H NMR spectrum (500 MHz) of ART A in DMSO-d_6 with a touch of DMSO is also presented as a reference. 1D ROESY experiment parameters were set as: SW 20 ppm; O1P 8.0 ppm; D1 1 sec; D16 0.0002 sec; P15 0.2 sec; NS 128.

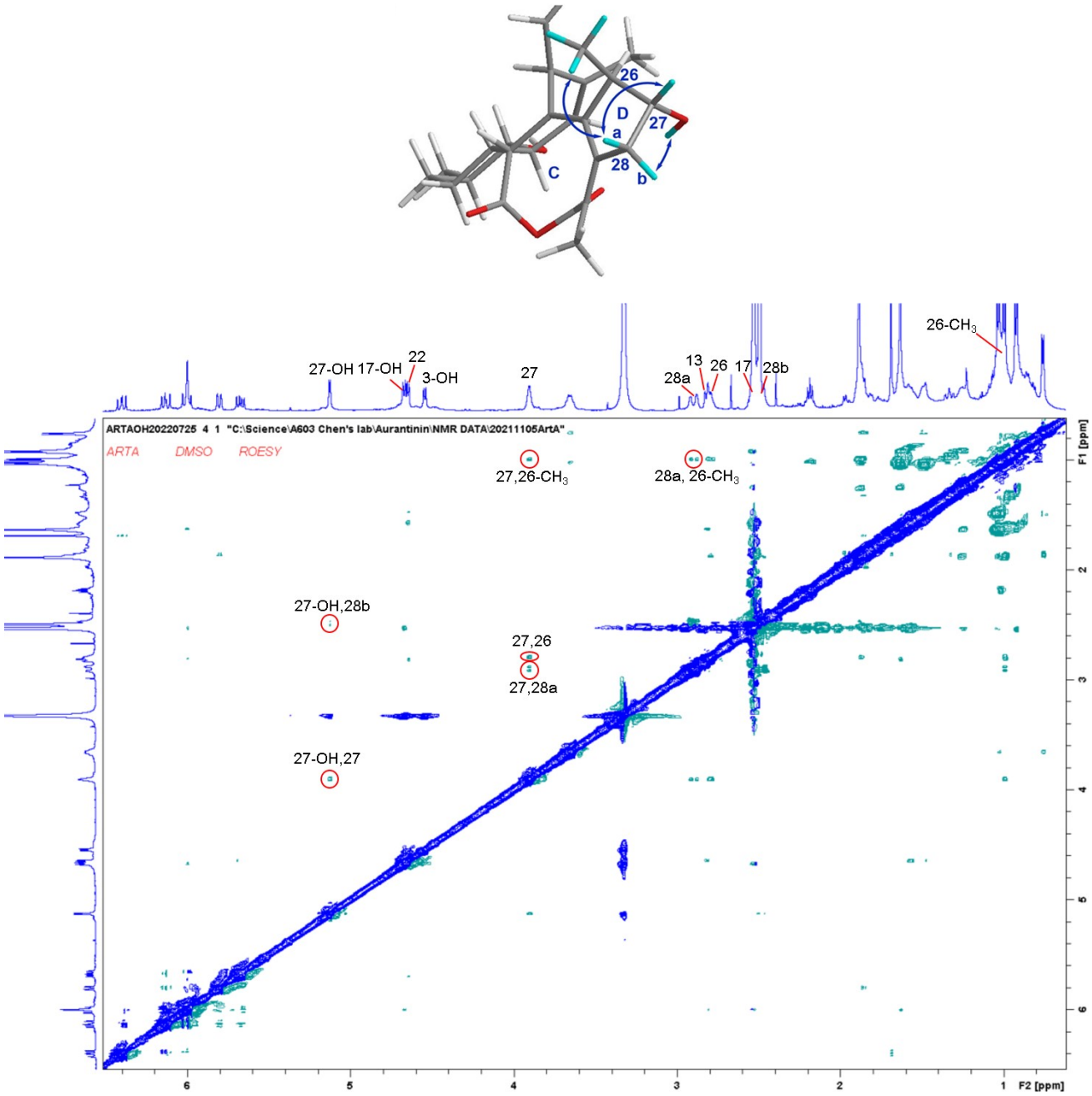

Fig. S13 ^{1}H-^{1}H ROESY spectrum (500 MHz) of ART A in DMSO-d_6 with a touch of DMSO.

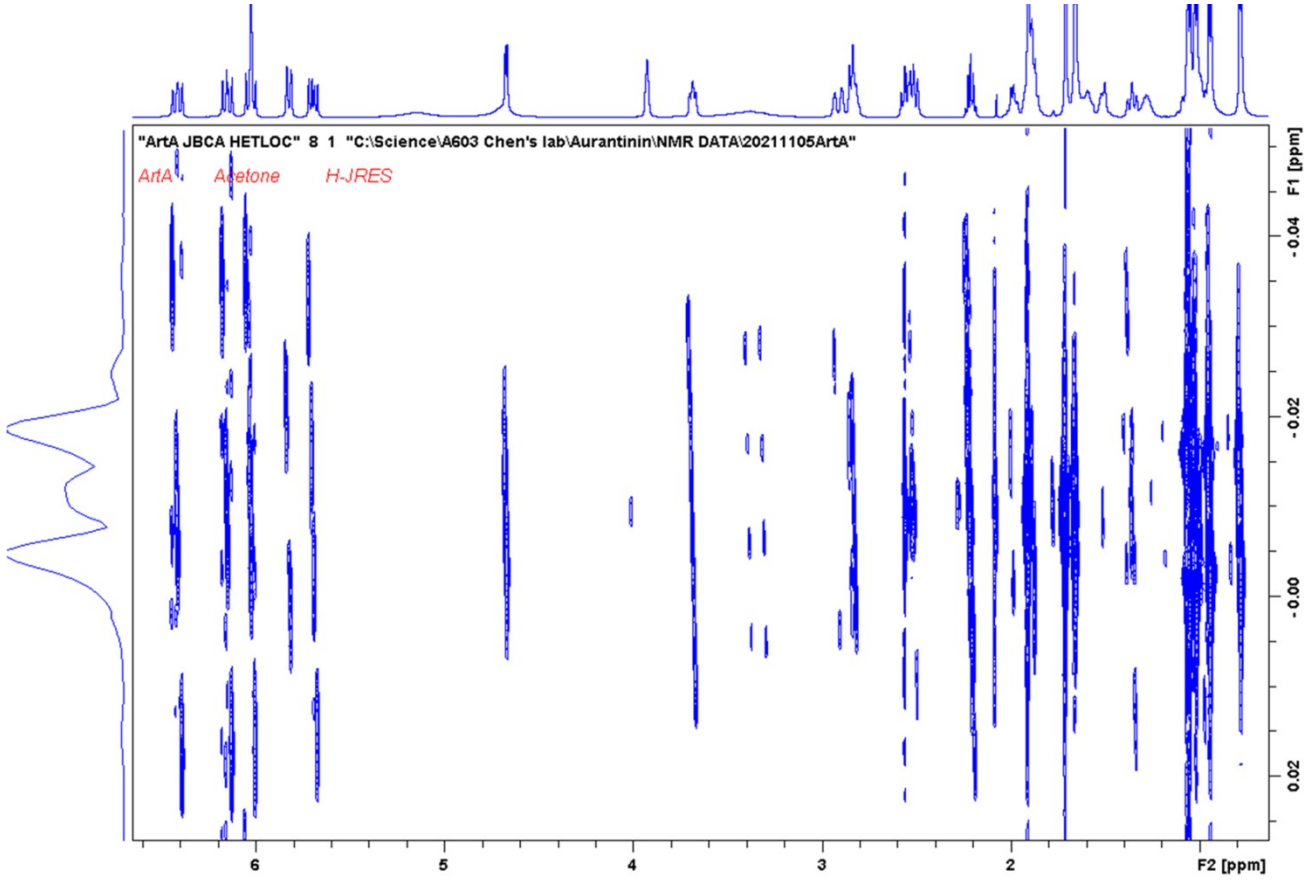

Fig. S14 2D *J*RES spectrum (500 MHz) of ART A in DMSO-d_6.

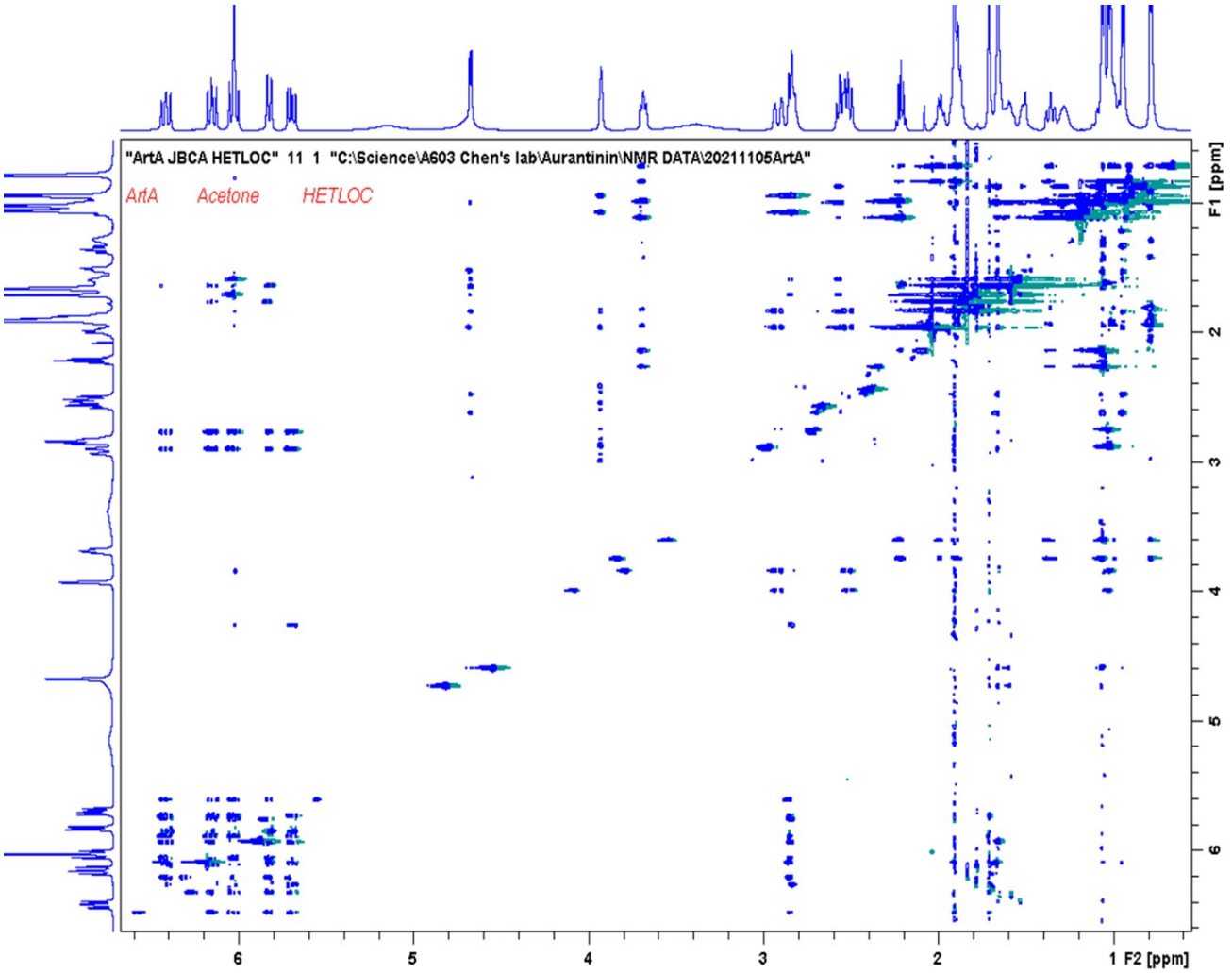

Fig. S15 HETLOC spectrum (500 MHz) of ART A in DMSO-d_6.

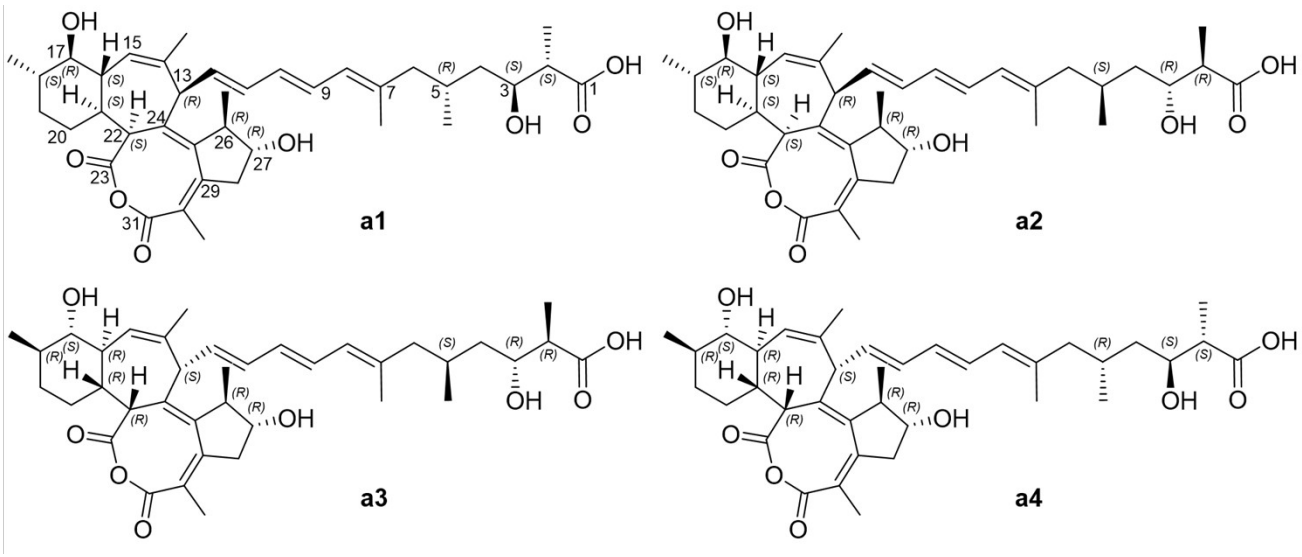

Fig. S16 Candidate stereoisomers of ART A.

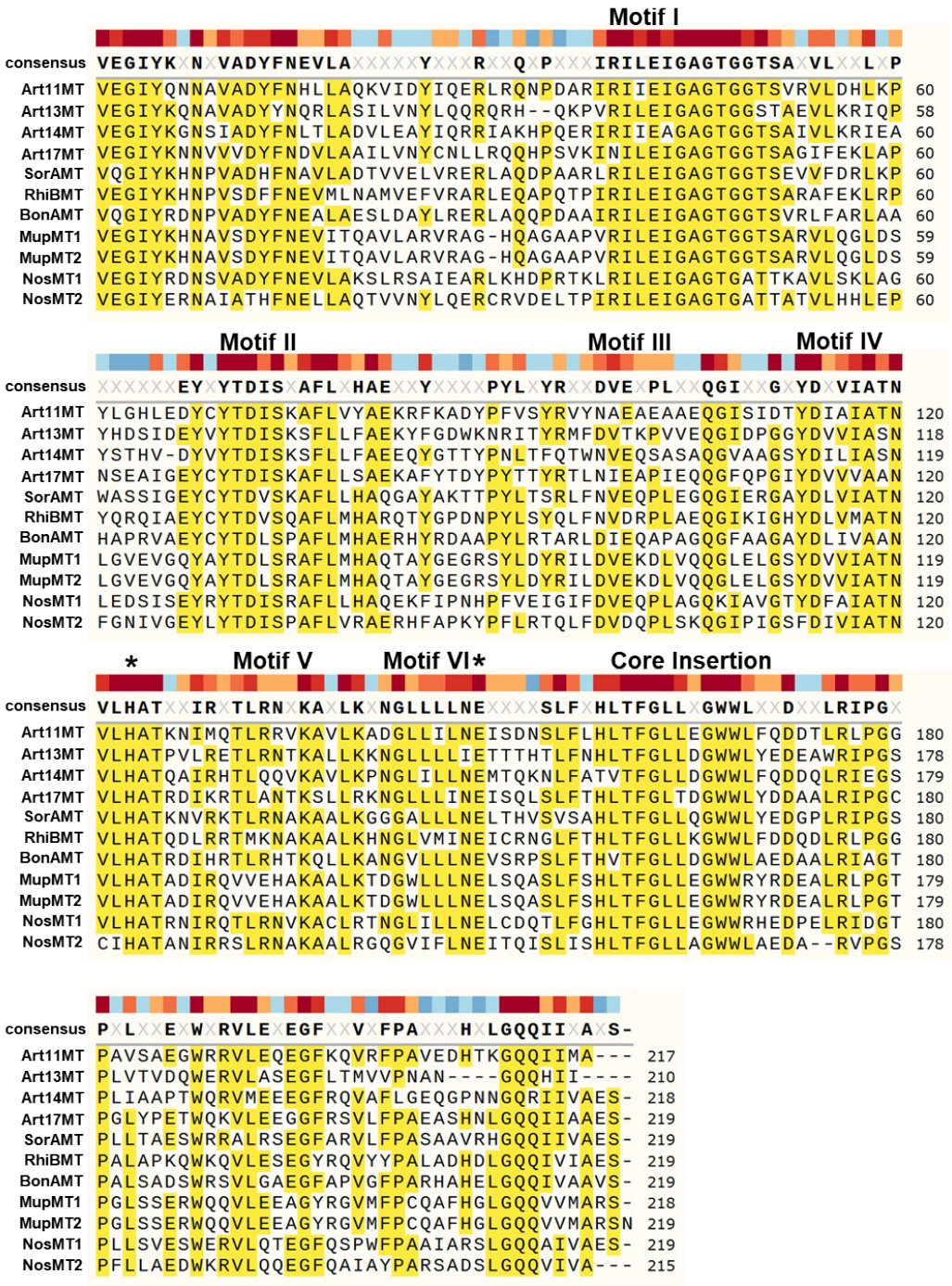

Fig. S17 Multiple sequence alignments of the MT domains from ART and the representative MT domains from *trans*-AT PKSs. The conserved motifs of MT domains are labeled on top and the catalytic dyad are indicated with asterisks. The sequence identity of the four ArtMT domains with the well-characterized BonAMT domain are 52.1% (Art11MT), 44.7% (Art13MT), 47.9% (Art14MT), and 55.7% (Art17MT), respectively.

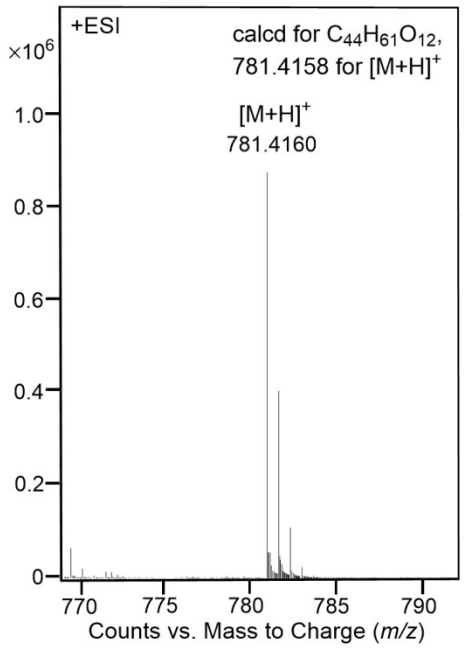

Fig. S18 HRESIMS spectrum of ART B.

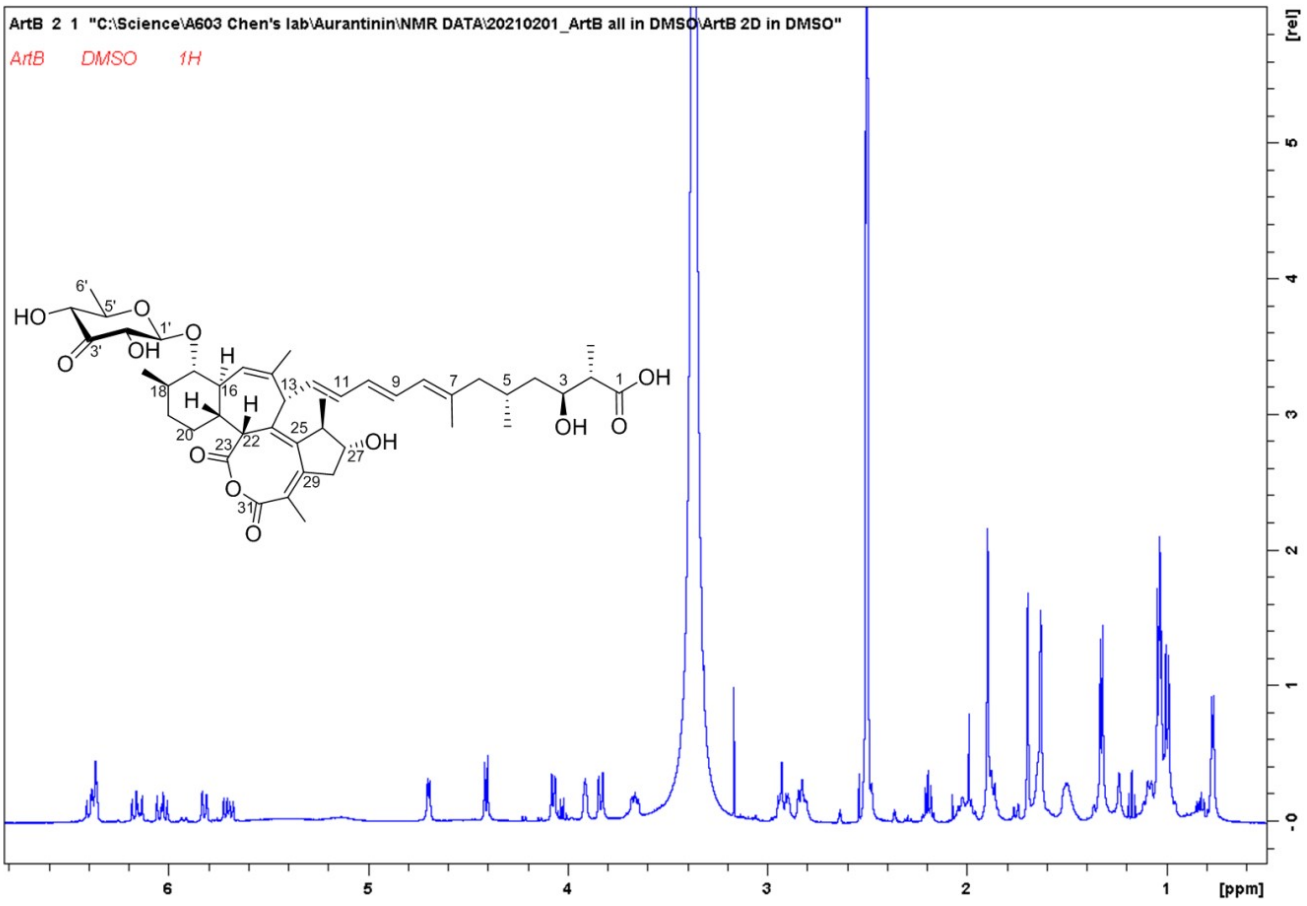

Fig. S19 ^{1}H NMR spectrum (500 MHz) of ART B in DMSO-d_6.

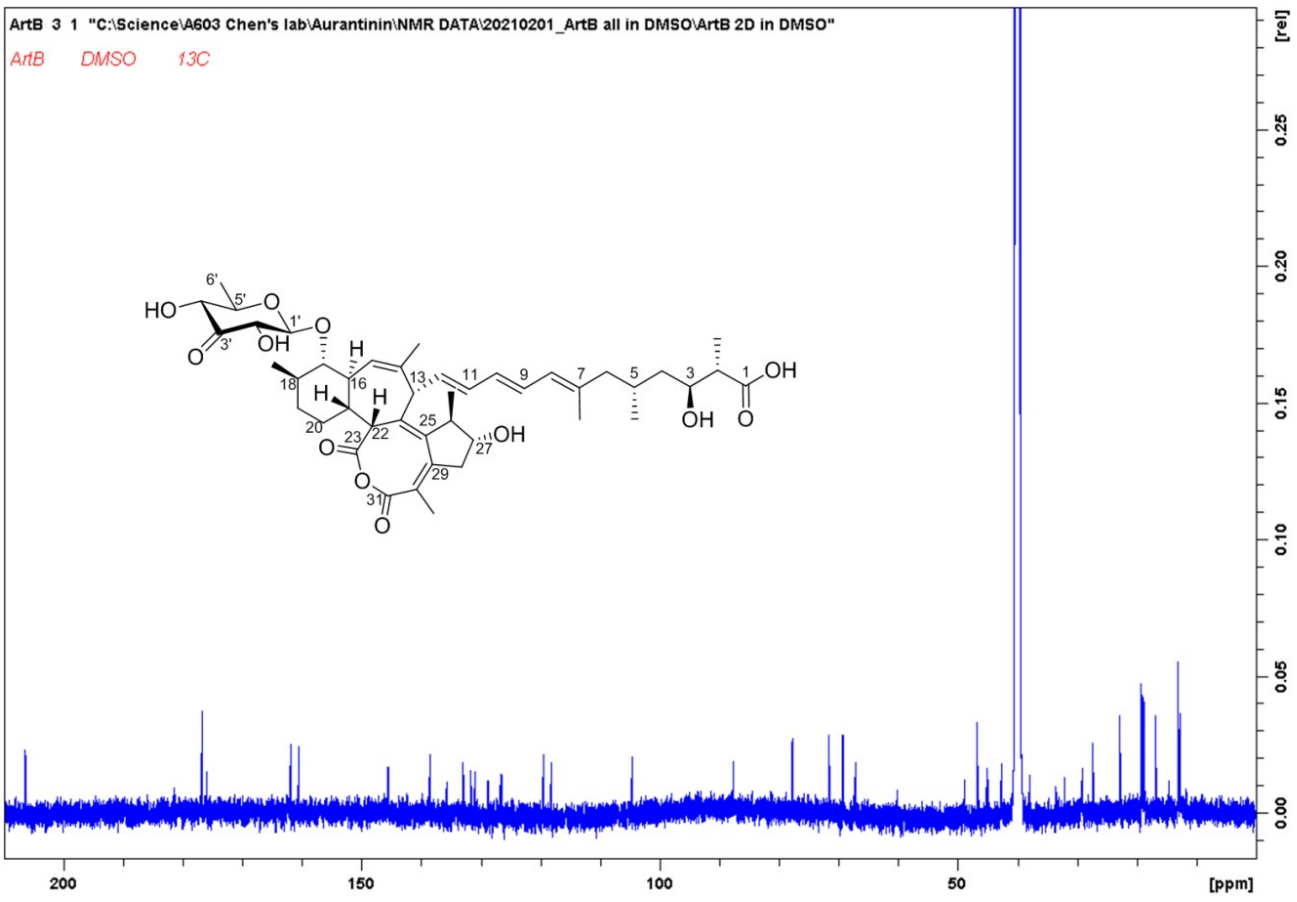

Fig. S20 ^{13}C NMR spectrum (125 MHz) of ART B in DMSO-d_6.

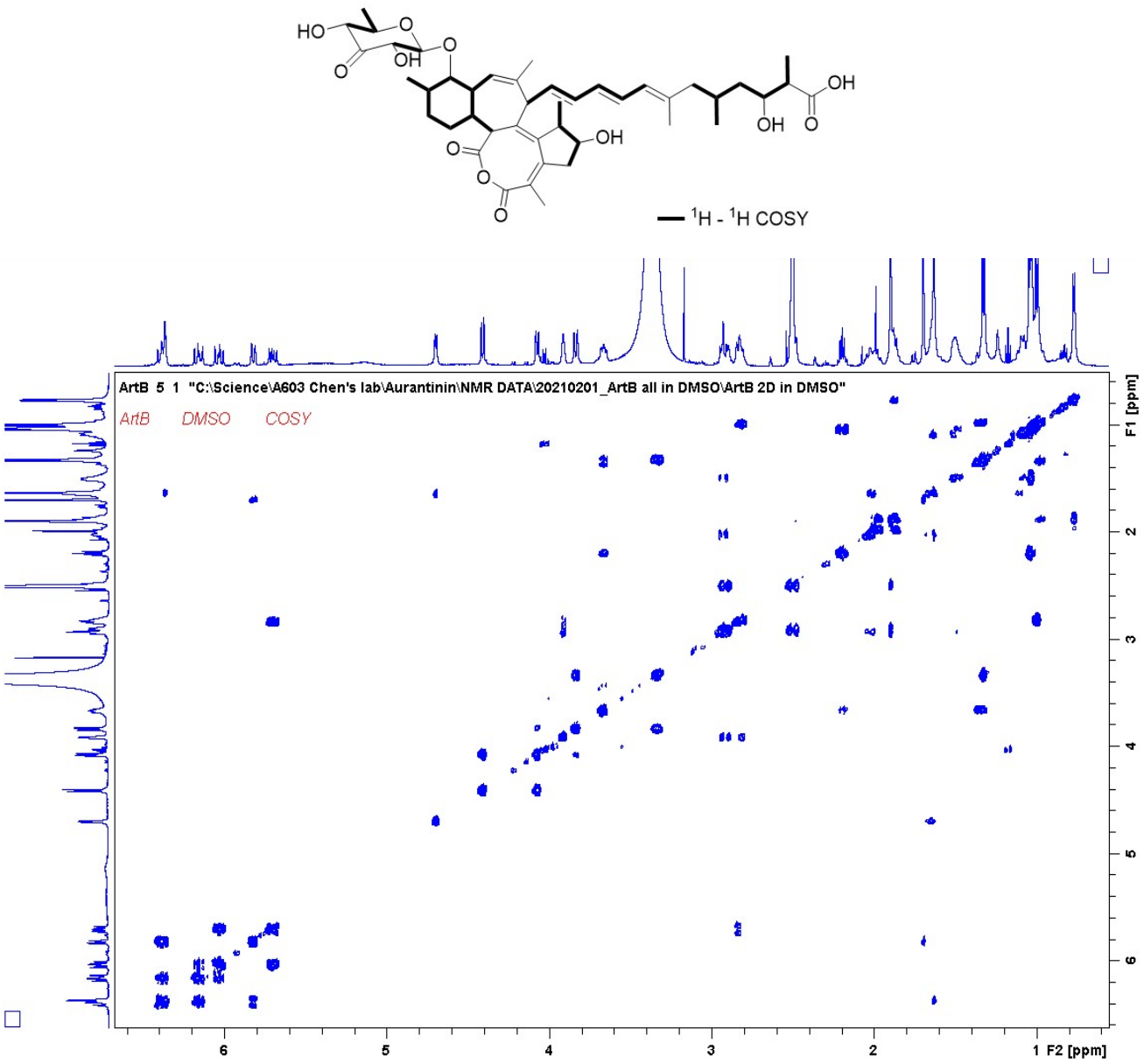

Fig. S21 ^{1}H-^{1}H COSY spectrum (500 MHz) of ART B in DMSO-d_6.

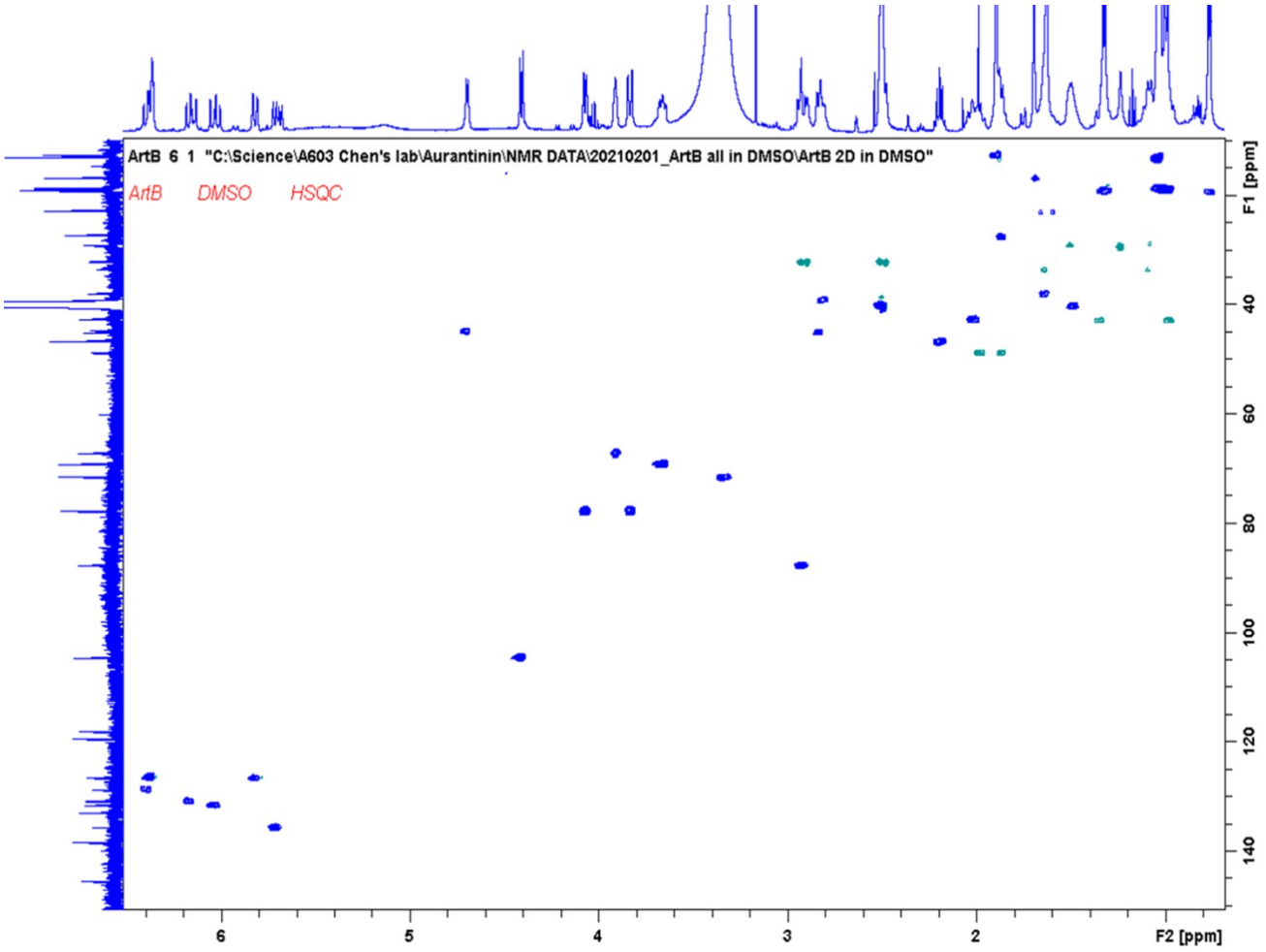

Fig. S22 ^{1}H-^{13}C HSQC spectrum (500 MHz) of ART B in DMSO-d_6.

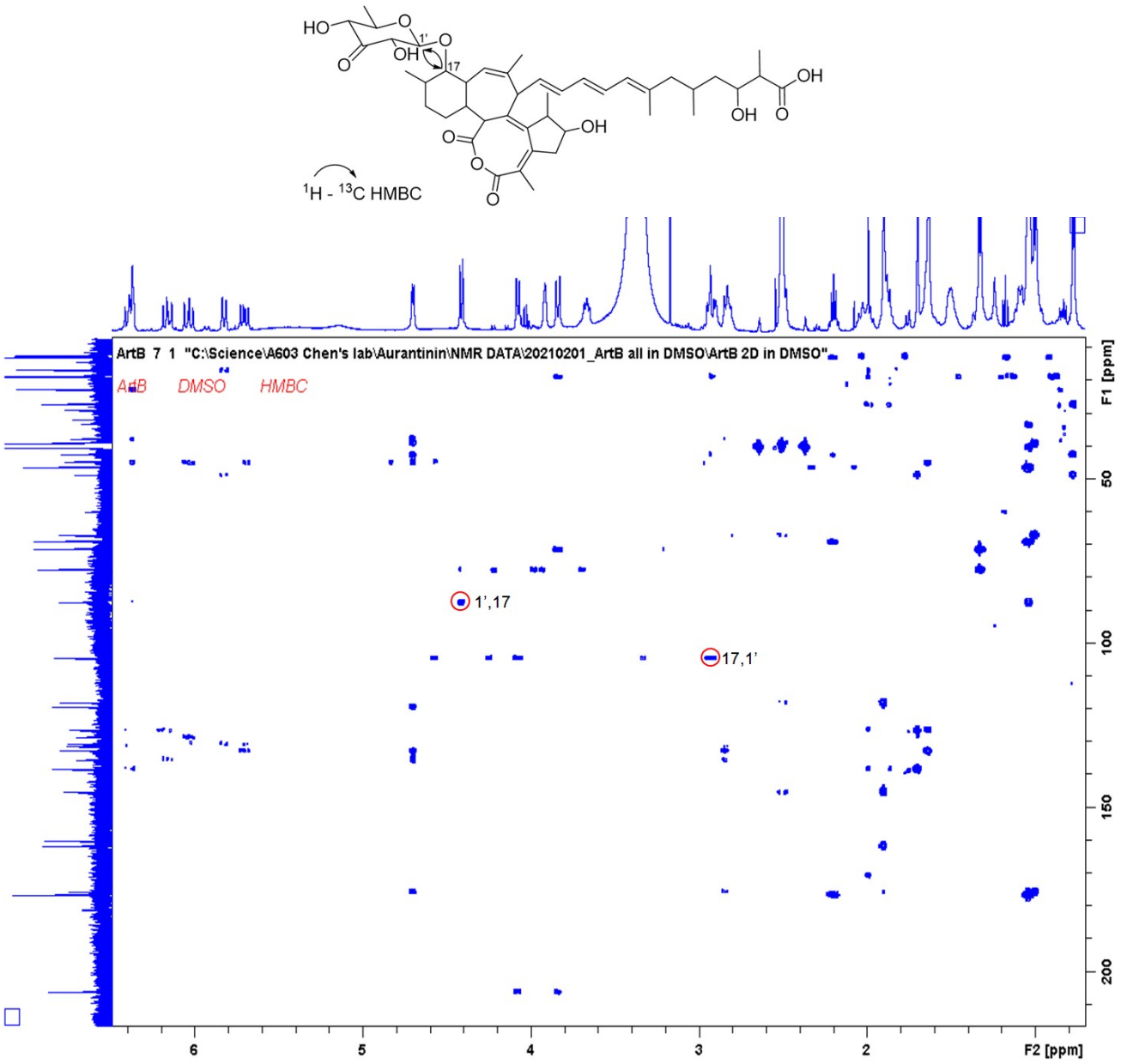

Fig. S23 ^{1}H-^{13}C HMBC spectrum (500 MHz) of ART B in DMSO-d_6.

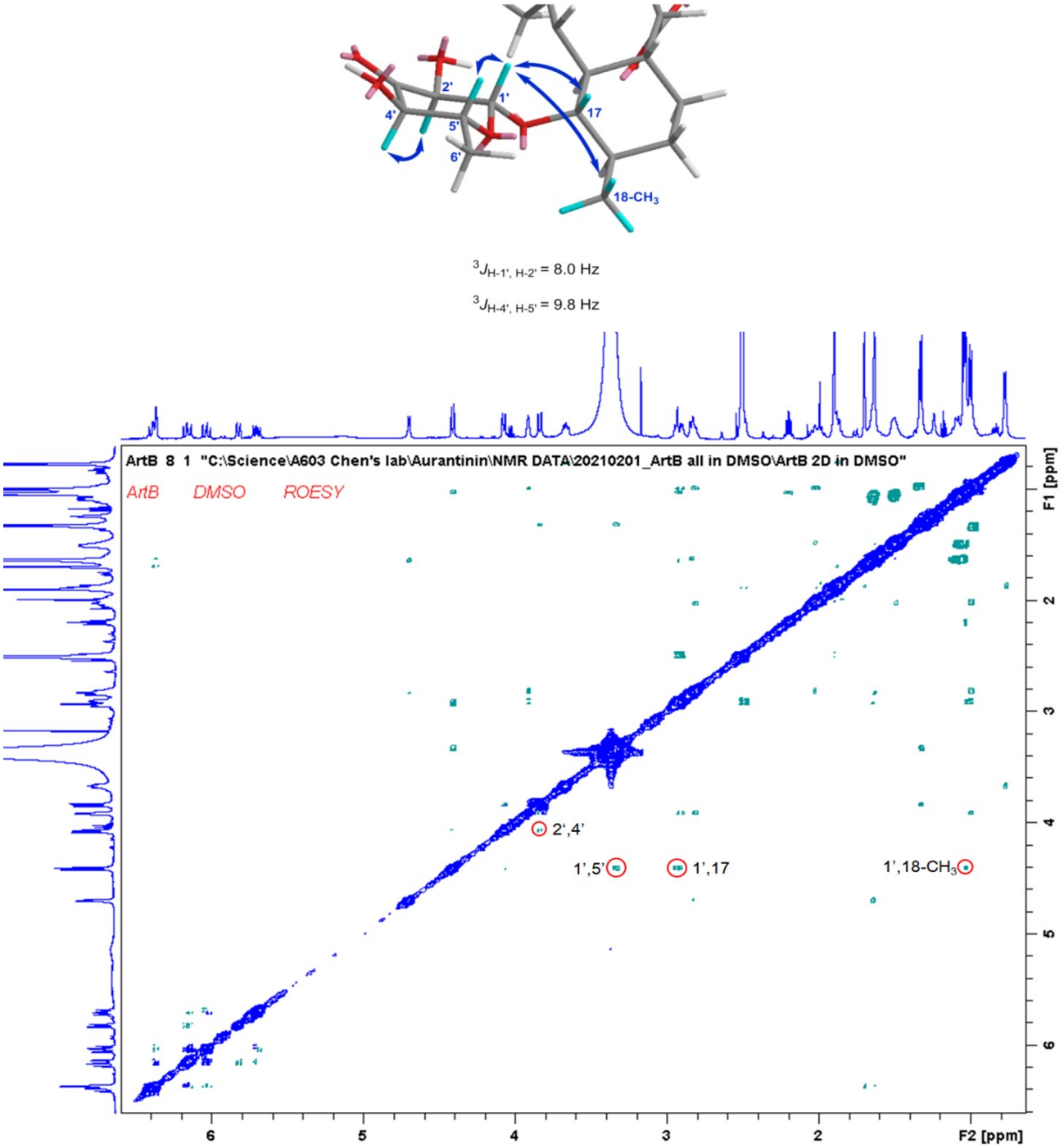

Fig. S24 ^{1}H-^{1}H ROESY spectrum (500 MHz) of ART B in DMSO-d_6.

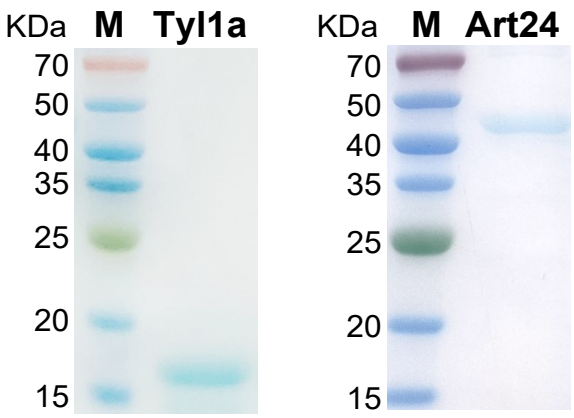

Fig. S25 SDS-PAGE analysis of Tyl1a and Art24.

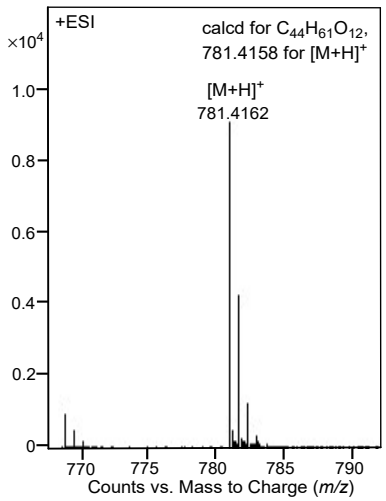

Fig. S26 HRESIMS analysis of the production of ART B in the Art24 assay.

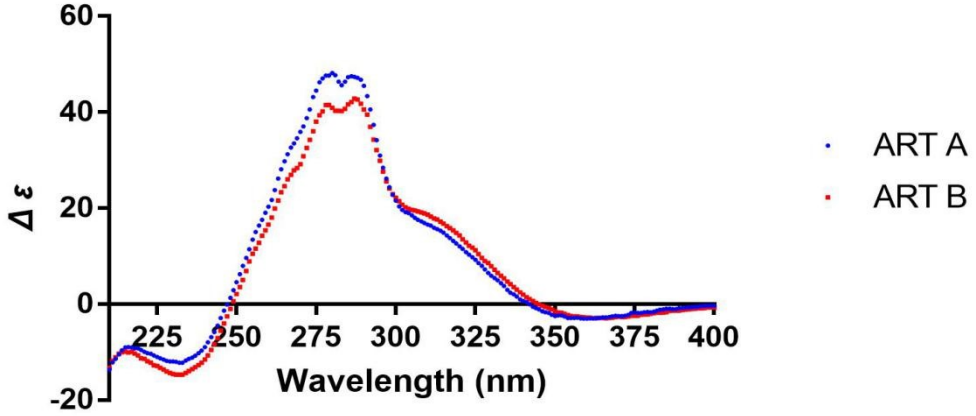

Fig. S27 Experimental CD spectra of ART A and ART B.

Table S1. Primers used in this study.

Primers	Sequences (5′ to 3′)*	Uses
24-L-F	aaagacataatcgatAAGCTTtcttatgcggtcaggtgaaatg	Amplification of the upstream region of *art24* (*Hin*dIII)
24-L-R	cccagcttcctcaaaggatttctctccttgattaaccaatgc	
24-R-F	gcattggttaatcaaggagagaaatcctttgaggaagctggg	Amplification of the downstream region of *art24* (*Hin*dIII)
24-R-R	taaactaccgcattaAAGCTTctgcataatctccgcctgaat	
28-24-F	tgccgcgcggcagcCATATGtcaaatgtgctgtttttaaacg	Amplification of *art24* (*Nde*I and *Bam*HI)
28-24-R	cggagctcgaattcGGATCCtcaggaaagaatttttttcttc	

*The designed restriction site in each primer is capitalized and underlined.

Table S2. ^{13}C NMR (125 M Hz) and ^{1}H NMR (500 M Hz) data of ART A and ART B in DMSO-d_6.

No.	ART B		ART A	
	δ_C(ppm)	δ_H(ppm, *J*=Hz)	δ_C(ppm)	δ_H(ppm, *J*=Hz)
1	176.8		176.5	
2	46.7	2.19, p, *J*=6.7	46.4	2.21, p, *J*=6.9
2-CH_3	13.1	1.04, d, *J*=6.7	12.7	1.06, d, *J*=6.9
3	69.3	3.67, ddd, *J*=9.8, 6.7, 2.3	68.9	3.69, m
3-OH				4.57, d, *J*=6.7
4	42.7	1.35 0.99	42.3	1.36, m (4a) 0.99, m (4b)
5	27.4	1.87	27.1	1.89, m
5-CH_3	19.2	0.77, d, *J*=5.9	18.9	0.78, d, *J*=5.9
6	48.9	1.98, m 1.87, m	48.5	1.99, m 1.89, m
7	138.5		138.1	
7-CH_3	16.9	1.70, s	16.5	1.71, s
8	126.7	5.82, d, *J*=11	126.4	5.83, d, *J*=11
9	128.8	6.39, dd, *J*=14.6, 11	128.5	6.42, dd, *J*=14.4, 11
10	130.9	6.16, dd, *J*=14.6, 10.7	130.6	6.15, dd, *J*=14.4, 10.7
11	131.7	6.03, dd, *J*=14.7, 10.7	131.2	6.03, m
12	135.7	5.70, dd, *J*=14.7, 8.5	135.3	5.70, dd, *J*=14.9, 8.4
13	45.1	2.84, m	44.9	2.85, m
14	132.9		133.5	
14-CH_3	22.8	1.63, s	22.8	1.66, s
15	126.5	6.37, s	125.6	6.02, s
16	42.7	2.02, m	44.2	1.92, m
17	87.7	2.93, m	78.1	2.56, m
17-OH				4.70, d, *J*=7.1
18	40.4	1.49, m	40.3	1.28, m
18-CH_3	18.8	1.03 d, *J*=6.3	18.9	0.95, d, *J*=6.3
19	33.6	1.64, m 1.10, m	33.2	1.66, m 1.06, m
20	29.1	1.51, m 1.24, m	29.0	1.51, m 1.08, m
21	38.0	1.64, m	37.4	1.59, m
22	44.9	4.70, d, *J*=5.1	44.5	4.67, d, *J*=5.2
23	175.9		176.1	
24	160.5		160.1	
25	119.5		119.0	
26	39.2	2.82, m	38.9	2.82, m

26- CH_3	18.9	1.00, d, *J*=6.8	18.58	1.02, d, *J*=6.8
27	67.2	3.92, m	66.9	3.93, m
27-OH				5.15, d, *J*=3.9
28	32.2	2.92, m 2.50, m	31.7	2.91, m 2.51, m
29	145.6		145.2	
30	118.2		117.8	
30-CH_3	12.7	1.90, s	12.4	1.91, s
31	161.9		161.5	
1′	104.7	4.41, d, *J*=8.0		
2′	77.9	4.08,dd, *J*=8.0, 1.6		
3′	206.4			
4′	77.7	3.84, dd, *J*=9.8, 1.6		
5′	71.6	3.34, m		
6′	19.0	1.33, d, *J*=6		

Table S3. The criteria of $^{3}J_{H,H}$ and $^{2,3}J_{C,H}$ values (Hz) for anti and gauche orientations in acyclic systems.

	$^{3}J_{H,H}$*		$^{2}J_{C,H}$*		$^{3}J_{C,H}$*	
	anti	gauche	gauche	anti	anti	gauche
oxygenation	large	small	large	small	large	small
none	9 to 12	2 to 4			6 to 8	1 to 3
mono	8 to 11	1 to 4	-5 to -7	0 to -2	6 to 8	1 to 3
di	7 to 10	0 to 3	-4 to -6	2 to 0	5 to 7	1 to 3

*Our manuscript refers to the criteria proposed in the reference as follows.

Nobuaki Matsumori, Daisuke Kaneno, Michio Murata, Hideshi Nakamura, and Kazuo Tachibana (1999) Stereochemical Determination of Acyclic Structures Based on Carbon−Proton Spin-Coupling Constants. A Method of Configuration Analysis for Natural Products. The Journal of Organic Chemistry. 64 (3), 866-876. DOI: 10.1021/jo981810k

Table S4. The results of the DP4+ analysis of ART A.

Functional		Solvent?		Basis Set		Type of Data	
mPW1PW91		PCM		6-311+G(d,p)		Shielding Tensors	
		DP4+	0.00%	0.00%	0.00%	100.00%	-
Nuclei	sp2?	xperimenta	Isomer 1	Isomer 2	Isomer 3	Isomer 4	Isomer 5
C	x	176.45	4.8514315	-1.8048927	-3.1220991	-1.2159904	
C		46.36	133.24295	139.076582	139.896087	138.973091	
C		68.94	112.175291	112.762952	113.854196	112.08375	
C		42.27	151.590824	144.363336	144.84809	145.08923	
C		27.06	149.518891	154.647889	158.374055	155.662532	
C		48.54	135.457843	144.716373	138.453469	135.489241	
C	x	138.09	37.2719412	35.02738	34.2842588	33.1620981	
C	x	126.38	52.2306327	59.1187294	58.9992697	54.7460083	
C	x	128.5	53.8325277	55.5380254	48.5097298	48.8753549	
C	x	130.57	50.9627535	55.7584547	58.0580709	58.0485095	
C	x	131.19	49.7176531	55.7732377	51.9785111	52.5782869	
C	x	135.3	47.4381007	45.8182866	54.0484757	52.9995846	
C		44.85	130.166891	129.119974	131.120351	132.041916	
C	x	133.5	43.2622122	42.9257747	41.5149994	42.6004514	
C	x	125.59	41.6045137	41.6842526	46.9527857	47.1008176	
C		44.22	141.989943	142.495335	140.52534	140.74323	
C		78.12	102.965894	102.712485	102.835897	102.970236	
C		40.27	145.032253	144.956016	144.227979	144.535793	
C		33.18	153.652636	153.329696	153.561956	153.460456	
C		29.01	154.597601	154.182305	154.434414	154.081741	
C		37.36	143.656712	143.053025	141.604601	142.246969	
C		44.5	124.79389	124.684049	122.578298	122.069616	
C	x	176.06	8.80604617	8.67239616	8.31379132	8.53207566	
C	x	160.1	36.9270493	36.7539749	31.7965606	31.8885466	
C	x	119.04	33.154029	33.2208651	35.1155193	35.2851687	
C		38.87	131.377223	132.006151	134.276206	133.681464	
C		66.9	109.810746	110.199973	105.957028	106.305954	
C		31.74	139.812561	139.36202	140.790221	140.662244	
C	x	145.21	19.6299959	19.9137949	21.3701799	21.8008917	
C	x	117.76	51.9712089	51.1486387	50.7181748	51.489218	
C	x	161.53	16.2326023	16.474404	15.3108144	15.2173573	
C		22.79	159.407483	159.236744	159.664655	159.837908	
C		18.95	168.324009	168.234973	168.54285	168.196338	
C		18.58	169.158721	168.917388	165.939171	165.464736	
C		12.69	177.127806	170.136982	169.888191	170.07916	
C		12.36	166.563506	166.540654	165.526073	165.622404	
C		18.86	164.79649	166.367735	167.487728	165.966128	
C		16.54	166.599736	160.274977	166.876159	169.461303	

Table S5. NMR data comparison of ART B sugar moiety with the other 3-keto sugars.

No.	ART B (DMSO-d_6)		ethyl-β-D-ribo-hex-3-ulopyranoside (MeOH-d_4)		methyl-β-D-ribo-hex-3-ulopyranoside (MeOH-d_4)		acetyl 2,4-di-O-acetyl-6-deoxy-β-D-ribo-hexopyran-3-uloside ($CHCl_3$-d_1)
	^{13}C	^{1}H	^{13}C	^{1}H	^{13}C	^{1}H	^{1}H
1′	104.7	4.41,d, *J*=8.0	105.6	4.36, d, *J*=7.8	106.8	4.27, d, *J*=7.9	5.78, d, ***J***= 8.5
2′	77.9	4.08,dd, *J*=8.0, 1.6	78.4	4.10, dd, *J*=7.8, 1.8	78.3	4.10, dd, *J*=7.9, 1.8	5.29, dd, *J*=8.5,1.1
3′	206.4		207.2		207.0		
4′	77.7	3.84,dd,*J*=9.8, 1.6	73.7	4.21, dd, *J*=10.1, 1.8	73.6	4.22, dd, *J*=10.1, 1.8	4.99, dd, ***J***=1.1, 10.3
5′	71.6	3.34, m	78.4	3.30	78.2	3.31, ddd, *J*=10.1,4.9, 2.1	3.81, dq, ***J***=10.3, 6.1
6′	19.0	1.33,d, *J*=6.0	62.6	3.78,dd, *J*=12.4, 5.0; 3.92,dd, *J*=12.4, 2.3	62.5	3.79, dd, *J*=12.1, 4.9; 3.94, dd, *J*=12.1, 2.1	1.37, d, *J*= 6.1

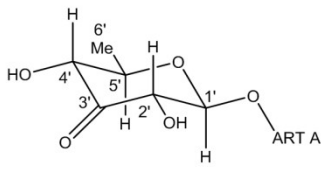

ART B

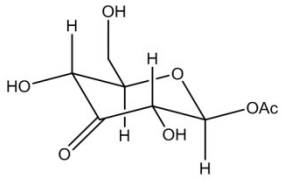

ethyl-β-D-ribo-hex-3-ulopyranoside

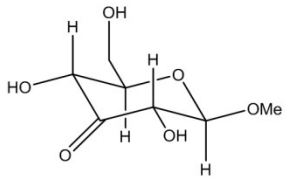

methyl-β-D-ribo-hex-3-ulopyranoside

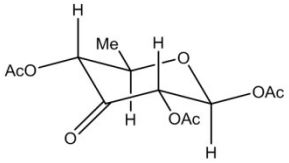

acetyl 2,4-di-O-acetyl-6-deoxy
-β-D-ribo-hexopyran-3-uloside